Dynamic modeling of turtle cortex stimulated by natural input

Jenner J. Joseph*
Department of Electrical and Systems
Engineering, Washington University
St. Louis, MO 63130
jenner@netra.wustl.edu

B. K. Ghosh**
Department of Electrical and Systems
Engineering, Washington University
St. Louis, MO 63130
ghosh@netra.wustl.edu

***Abstract*— The visual cortex of a freshwater turtle, when stimulated by a pattern of light, produces waves of activity that have been both recorded experimentally and simulated using a model cortex. In this paper, the goal is to predict the response of the model cortex when the input pattern is a natural source. The basic procedure is to encode both the input and the output signals using a suitable choice of spatial and temporal basis functions. The encoding process generates a vector time series of coefficients (temporal strands) in a suitable lower dimensional beta-space. Finally, a linear system is identified that best fits the input strand to the output strand.**

I. Introduction to the cortical wave generation

Extracellular recordings [7] and experiments with voltage sensitive dyes [11], [10], [12] have established the fact that the visual cortex of freshwater turtles produces waves of activity as a result of an input pattern of visual activity. Experimentally, these patterns have been generated for inputs restricted to a stationary flash of light localized at various parts of the visual field or a moving flash with constant velocity. A large scale model [9], [8] of the turtle visual cortex has been constructed that has the ability to simulate cortical waves with the same qualitative features as the cortical waves seen in experimental preparations. The model cortex can now be used to generate simulated output to many and perhaps more complex input stimuli. In an earlier paper, Joseph and Ghosh [5] used harmonic inputs of the form

$$u_r(t) = k_r cos(\omega_r t),$$

to record the model cortical output. The corresponding beta strands were generated using principal component analysis. Application of Volterra theory of nonlinear systems [5], with $u_r(t)$ as the input to the system, enabled identification of the corresponding Volterra kernels. This paper is an extension of [5], where the input is now chosen as a natural stimulus. In so doing, we are no longer able to use the harmonic probing technique of Boyd et al [2]. The input to the cortex is now distributed both in space and time. In order to be consistent with the model cortex [9], the spatial dimension of the input signal is chosen to be one.

*Research was partially supported from NSF grant ECS-9976174
**Research was partially supported from NSF grants ECS-9976174, and ECS-0323693

II. Encoding the turtle's visual input

A turtle's visual field has a high level of acuity along a horizontal axis, called the *visual streak*. In this paper, we propose to restrict the visual input to the visual streak by considering a horizontal cross section of the field of view. Figure 1 illustrates an example of a typical such cut. 201 contiguous positions are chosen corresponding to the 201 lateral geniculate nucleus (LGN) neurons in our model cortex. We compute $u(x,t)$, the appropriate intensity function at each position. The function $u(x,t)$ is smoothed in time and we obtain $\bar{u}(x,t)$. Samples of these functions are shown in Figure 2, for a suitable natural video sequence. We now expand $\bar{u}(x,t)$ in terms of its principal components as follows

$$\bar{u}(x,t) = \sum_{i=1}^{N} \alpha_i(t)\psi_i(x).$$

We may further expand the $\alpha_i(t)$ as

$$\alpha_i(t) = \sum_{j=1}^{q} \beta_j \phi_j(x),$$

where the $\phi_j(x)$ are the 'principal temporal modes' and the $\beta_j(t)$ are the corresponding coeficients. These will be addressed in greater detail in Section III. We propose to use these q-dimensional β vectors as input to our dynamic model.

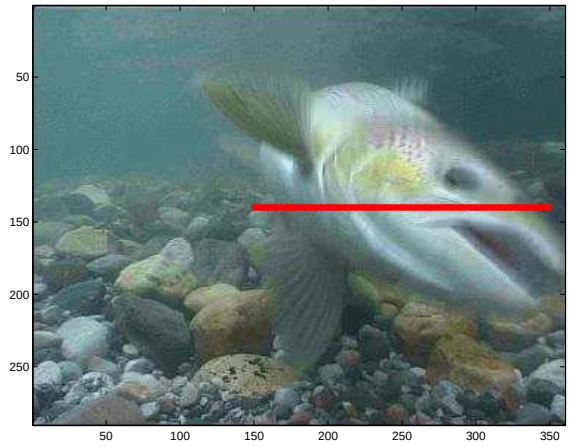

Fig. 1. An example of a natural scene used which illustrates a typical horizontal cut. 201 contiguous spatial positions are selected. The image intensity is observed, in time, from each of these fixed locations.

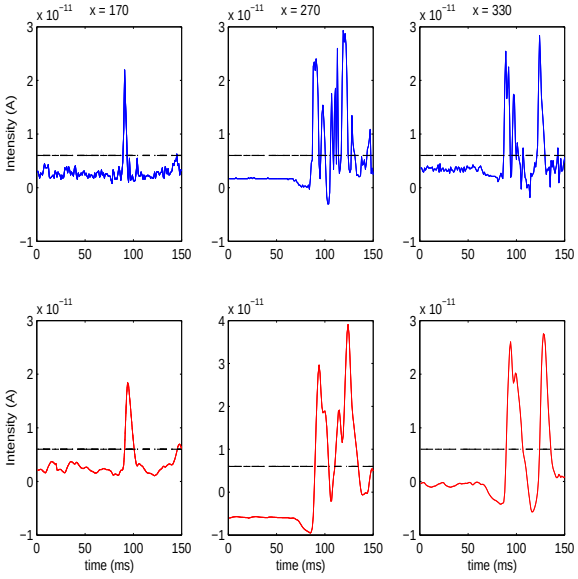

Fig. 2. Scaled image intensity, $u(x,t)$, and its smoothed counterpart, $\bar{u}(x,t)$, corresponding to three different positions along the same horizontal cut. Spatial positions chosen were $x = 170$, $x = 270$, and $x = 330$, all at $y = 53$ based on the coordinate system represented in Fig 1. The threshold at which the model LGN neurons fire was experimentally found to be approximately 6 picoamperes and is indicated by the dashed line.

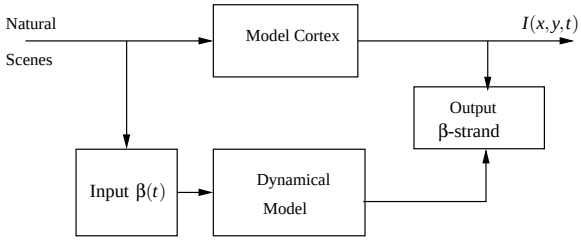

Fig. 3. Block diagram of the overall scheme.

III. The Beta Strand Representation of the Waves

The visual cortex of freshwater turtles contains three layers. Our model [9] assumes that the three layers are projected onto a single plane. Each neuron is represented by a multicompartmental model based on the anatomy of the turtle neurons. Each compartment is modeled by a standard membrane equation and implemented in GENESIS [1]. A set of 201 geniculate neurons are linearly arranged as described in [9]. Through the synaptic interactions between the geniculate, pyramidal, stellate, and horizontal neurons, the cortex is activated. We are primarily concerned with the pyramidal neurons, and their responses are visualized as a spatiotemporal signal $I(x,y,t)$ and displayed as a movie. Selected views from a few typical movies are displayed in Figure 4. It should be noted here that through the encoded signal, the model cortex not only discriminates between inputs from different natural scenes, but also between inputs from neighboring cuts of the same scene. In Figure 4, the first two columns show the cortical response to inputs that are only four pixels apart. Once the signal $I(x,y,t)$ has been obtained, it can be represented using principal component analysis as

$$I(x,y,t) = \sum_{i=1}^{p} \alpha_i(t)\, M_i(x,y), \qquad (1)$$

where $M_i(x,y)$ are the 'principal spatial modes' obtained by considering the response of the cortex to 50 different inputs each corresponding to a different horizontal cut from the natural scene. In our model, $p = 679$ is the number of pyramidal cells, and this is the number of $\alpha(t)$ coefficients present. The coefficient vector $\alpha(t) = (\alpha_1(t), \alpha_2(t), \ldots, \alpha_p(t))$ can be further expanded using 'principal temporal modes' $\phi_i(t)$ as

follows:

$$\alpha(t) = \sum_{i=1}^{q} \beta_i \, \phi_i(t). \tag{2}$$

The q dimensional β-vector represents the spatio-temporal signal $I(x,y,t)$ over the entire spatial dimension of the cortex and over a time window. The time window has been allowed to slide, leading to a sequence of β-vectors called a 'beta strand' (see Figure 8). Note that each strand is a lower dimensional representation of the cortical response with respect to a set of spatial and temporal basis functions and has already been introduced by Du et al. [3]. Here, each time window is chosen to be $T = 10\,ms$ in width and the time step considered is $dT = 2\,ms$.

IV. On the problem of dynamic modeling

Our dynamic modeling approach involves treating the β strands, obtained from the natural scenes, as input to a linear time-invariant dynamical system. Of particular interest is the model format discussed in [4] and [6], in which the current output vector is expressed as a linear combination of past outputs, $y(t)$, and past inputs, $u(t)$. We consider the case where the input $u(t)$ is an m-dimensional vector and the output $y(t)$ is a p-dimensional vector. It is of the form

$$A(q^{-1})y(t) = B(q^{-1})u(t) + e(t); \quad t \geq 0 \tag{3}$$

where

$$A(q^{-1}) = I + A_1 q^{-1} + \cdots + A_{n_a} q^{-n_a} \tag{4}$$

$$B(q^{-1}) = B_1 q^{-1} + \cdots + B_{n_b} q^{-n_b} \tag{5}$$

Here, I and the A_i are $p \times p$ matrices and the B_i are $p \times m$ matrices whose entries are polynomials in the delay operator q^{-1}. n_a represents the number of output samples that are included in (4) and n_b represents the number of input samples that are included in (5). The model may now be concisely expressed as

$$y(t) = \Theta^T \phi(t) + e(t) \tag{6}$$

where

$$\Theta = [A_1 \cdots A_{n_a} B_1 \cdots B_{n_b}]^T$$

is a $[n_a \cdot p + n_b \cdot m] \times p$ matrix, and

$$\phi(t) = [-y(t-1) \cdots -y(t-n_a) u(t-1) \cdots u(t-n_b)]^T$$

is a $[n_a \cdot p + n_b \cdot m]$-dimensional vector. The multivariable least squares algorithm can then be applied.

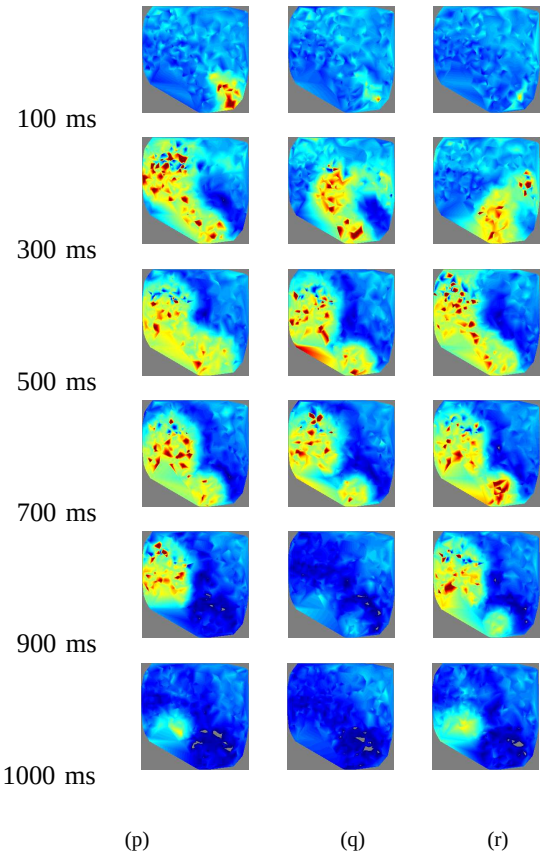

Fig. 4. Selected views of turtle cortical waves which represent the response to stimuli from three horizontal cuts. The first two columns, (p) and (q), are from the same natural scene with cuts made at y = 143 and at y = 147 respectively. The last column, (r), is from a different movie with the cut made at y = 62. Cortical discrimination is evident from these snapshots.

V. Results

For this problem, input dimension $m = 3$ and output dimension $p = 3$ were chosen. The significance here is that almost all information contained in the input and output β-vectors is retained if $q = 3$ in (2). As a matter of fact, the fourth β component is typically less that 10% of the first. The model parameters were estimated from an input-output pair generated from spatial location: $x = [\,149, 350\,]$ and $y = 53$ (see Figure 1 for reference). Figures 5, 6, and 7 show how the model simulated output compares to the real output data. We define the model's goodness of fit, F as

$$F = \left[1 - \frac{\| y - \hat{y} \|}{\| y - \bar{y} \|}\right] \times 100$$

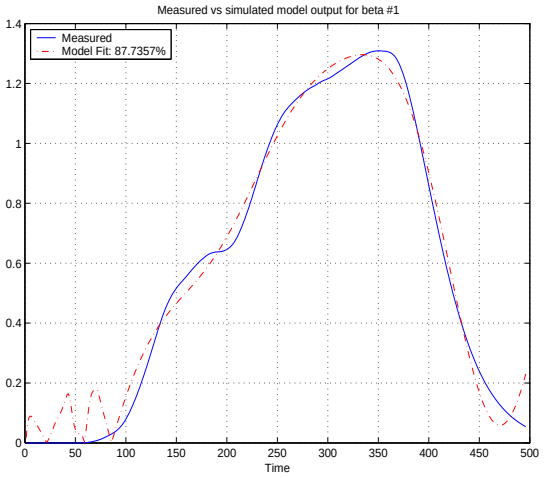

Fig. 5. The most dominant beta component, β_1. The model was able to fit the true output to 87.7357 % accuracy.

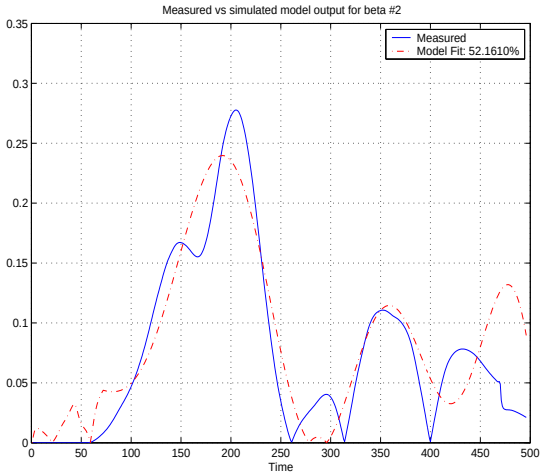

Fig. 6. The second most dominant beta component, β_2. The model was able to fit the true output to 52.1610 % accuracy.

and the figures indicate how good a job the model does at predicting each output vector. Clearly, the importance of the accuracy of the model's prediction ranges from most important in Figure 5 to least important in Figure 7 for reasons already mentioned. Figure 8 shows how the three-dimensional β strands compare. The model does a very good job of prediction in this scenario as evidenced by the 87.6479% goodness of fit. Since model validation is of great importance, and we follow some general methods mentioned in [6]. To see how much of the data is unexplained by the model, we analyze the residuals. We consider the autocorrelation

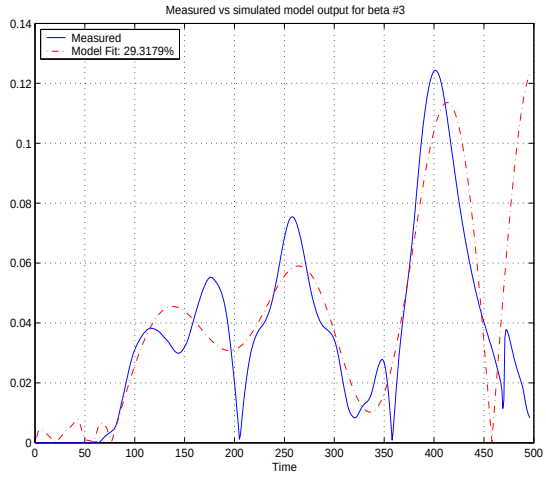

Fig. 7. The third most dominant beta component, β_3. The model was able to fit the true output to 29.3179 % accuracy.

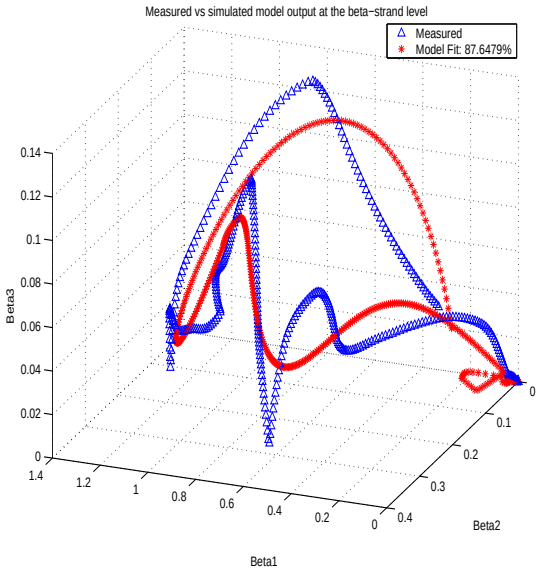

Fig. 8. Strands corresponding to the first three most dominant β components in time plotted as the time window of a given width ($T = 10\ ms$) is allowed to slide along the time axis every $dT = 2\ ms$. The model prediction was able to fit the true output strand to 87.6479 % accuracy.

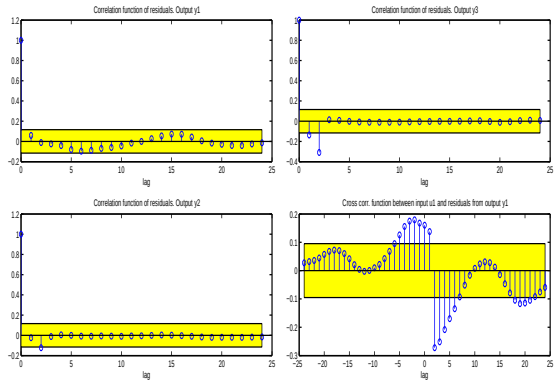

Fig. 9. From top to bottom and then from left to right, this figure shows the autocorrelation of the three e_i vectors as well as the cross-correlation between e_1 and u_1.

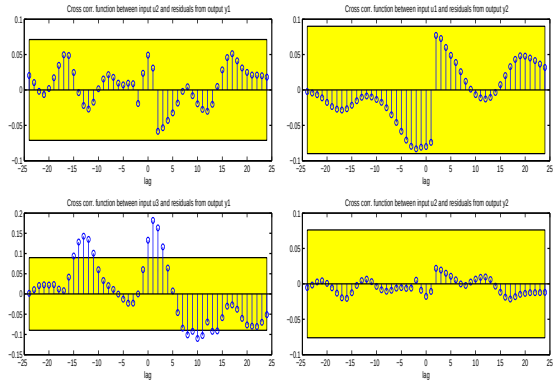

Fig. 10. From top to bottom and then from left to right, this figure shows the cross-correlation between e_1 and u_2, e_1 and u_3, e_2 and u_1, and e_2 and u_2.

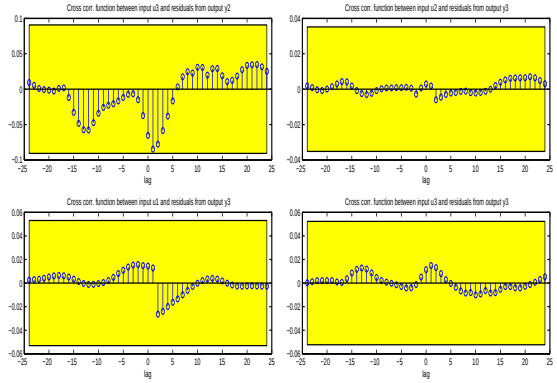

Fig. 11. From top to bottom and then from left to right, this figure shows the cross-correlation between e_2 and u_3, e_3 and u_1, e_3 and u_2, and e_3 and u_3.

of the system disturbance, e_i and the cross-correlation between the e_i and the inputs, u_j from Equation 3. Figures 9, 10, and 11 show the autocorrelation and cross-correlation functions as well as 99% confidence intervals for these functions. The system disturbance is assumed to be white and independent of the u_j. In general, one rejects a model in which the correlation functions range significantly outside of the confidence interval. Thus, Figures 9, 10, and 11 clearly demonstrate that the model gives a good representation of the system. Shortly, we plan to advance the model to predict unknown data within a given range reasonably well, if at all possible.

VI. REFERENCES

[1] J. M. Bower and D. Beeman. *The Book of Genesis*. TELOS, Santa Clara, 1998.

[2] S. Boyd, Y. S. Tang, and L. O. Chua. Measuring volterra kernels. *IEEE Trans. on Circuits and Systems*, 30(8):571–577, 1983.

[3] X. Du and B. K. Ghosh. Decoding the position of a visual stimulus from the cortical waves of turtles. In *Proc. of the American Control Conference*, pages 477–482, 2003.

[4] G. C. Goodwin and K. S. Sin. *Adaptive Filtering Prediction and Control*. Prentice-Hall, New Jersey, 1984.

[5] J. Joseph and B. K. Ghosh. A volterra approach to dynamic modeling of the visual cortex. In *Proc. of the American Control Conference*, pages 3579–3584, 2003.

[6] L. Ljung. *System Identification: Theory for the User*. Prentice-Hall, New Jersey, 1987.

[7] P. Z. Mazurskaya. Organization of receptive fields in the forebrain of emys orbicularis. *Neurosci. Behav. Physiol.*, 7:311–318, 1974.

[8] Z. Nenadic, B. K. Ghosh, and P. Ulinski. Modeling and estimation problems in the turtle visual cortex. *IEEE Trans. on Biomedical Engineering*, 49:753–762, 2002.

[9] Z. Nenadic, B. K. Ghosh, and P. Ulinski. Propagating waves in visual cortex: A large scale model of turtle visual cortex. *J. of Computational Neuroscience*, 14:161–184, 2003.

[10] K. A. Robbins and D. M. Senseman. Visualizing differences in movies of cortical activity. *IEEE*

Trans. Visualization Compt. Graphics, 4:217–224, 1998.

[11] D. M. Senseman. Correspondence between visually evoked voltage sensitive dye signals and activity recorded in cortical pyramidal cells with intracellular microelectrodes. *Vis. Neurosci.*, 13:963–977, 1996.

[12] D. M. Senseman and K. A. Robbins. Modal behavior of cortical neural networks during visual processing. *J. Neuroscience*, 19:1–7, 1999.